SCIENTIFIC REP🛇RTS

OPEN

Autophagy and mitochondrial dysfunction in adjuvant-arthritis rats treatment with resveratrol

Junqiang Zhang[1,*], Xianbin Song[2,*], Wei Cao[1,*], Jinseng Lu[1], Xiaoqing Wang[2], Gaoyuan Wang[3], Zhicheng Wang[4] & Xiaoyu Chen[1,*]

Resveratrol is a polyphenol derivatives which exhibits a pro-apoptotic effect in a variety of human cancers by triggering mitochondria apoptosis pathway and autophagy. However, there are scarcely reports on its apoptosis-promoting effect in abnormal proliferation fibroblast-like synoviocytes (FLSs). In this study, we investigated the underlying mechanism and apoptosis-inducing effects of resveratrol on the abnormal proliferation of FLSs in adjuvant-arthritis (AA) rats. Since using resveratrol for 12 days resulted in a significant decreasing the swelling degree of the paw, reducing malondialdehyde (MDA) content and enhancing superoxide dismutase (SOD) activity, antioxidant capacity, glutathione peroxidase and glutathione reductase ratio in AA rats. Moreover, we found that $5\,\mu M H_2O_2$ could increase cells viability, Beclin1, LC3A/B, MnSOD, SIRT3 protein expression in FLSs. But, resveratrol could reverse these effects by changing mitochondrial membrane potential ($\Delta\psi m$) to promote mitochondrial reactive oxygen species (mtROS) generation in $5\,\mu M H_2O_2$-treatment FLSs. These results suggest that oxidative stress existed in AA rats. Resveratrol could suppress oxidative stress in AA rats and increase mtROS production by reducing autophagy protein Beclin1, LC3A/B and oxidative stress protein MnSOD to promoted the apoptosis of FLSs. Thus, targeting of mtROS may be a crucial mechanism of resveratrol confers patients with rheumatoid arthritis.

Rheumatoid arthritis (RA) is a chronic systemic autoimmune disease characterized by persistent fibroblast-like synoviocytes (FLSs) proliferation with inflammatory cell infiltration and joint destruction[1]. Currently, adjuvant-induced arthritis (AA) rats are the most widely used arthritis models in academia and industry[1]. AA, which consist of paraffin oils, mannide monooleate, and heat-killed mycobacteria (Mb), known as complete Freund's adjuvant (CFA), is an experimental model of rheumatoid arthritis[2]. Some evidences show that FLSs exhibits tumor like growth, which is manifested as lack of contact inhibition[3]. Inflammatory cytokines such as tumor necrosis factor alpha (TNF-α), interleukin-6 (IL-6) and interleukin-1 beta (IL-1β) were significantly increased in patients with RA[4]. Some evidences indicated that over production of proinflammatory cytokines stimulated neutrophils and activated macrophages secreting ROS to the synovial fluid, which may act as mediators of synovial hyperplasia[5,6]. So promoting the apoptosis of FLSs, which may transform tissue composition and homeostasis, affecting the pathogenesis of RA.

Reactive oxygen species (ROS) such as superoxide anion ($O_2\bullet^-$), and hydroxyl radical (OH•), Hydroperoxyl (HO$_2$•), Peroxyl (ROO•), Alkoxyl (RO•), hydrogen peroxide (H_2O_2), plays a role in various biological processes including proliferation, Oxidative Stress, autophagy, apoptosis, tumor development[7–9]. Intracellular 90% ROS was produced by mitochondria in physiological conditions[10]. That Prolonged exposed in low levels of ROS may induce somatic mutations and cancer progression could contribute to acquire a malignant phenotype[11]. But, high levels of ROS lead to DNA and protein damage, lipid peroxidation, apoptosis even necrosis[12]. The enzymatic antioxidant defences mainly include Superoxide Dismutase (SOD), Glutathione Peroxidase (GSH-PX) and glutathione reductase (GR) in the body[12]. Superoxide or superoxide anion can be dismutated to H_2O_2 in a reaction catalyzed by superoxide dismutase (SOD)[13]. GSH-PX can promote the formation of glutathione (GSH) and H_2O_2 reaction to produce H_2O and glutathione disulfide (GSSG). Under the catalysis of glutathione reductase (GR),

[1]Department of Histology and Embryology, Anhui Medical University, Hefei 230032, China. [2]Basic Medicine, Anhui Medical College, Hefei 230601, China. [3]Department of Orthopaedic, the First Affiliated Hospital of Anhui Medical University, Hefei 230031, China. [4]Department of Laboratory Medicine, Huashan Hospital, Shanghai Medical College, Fudan University, Shanghai 200040, China. *These authors contributed equally to this work. Correspondence and requests for materials should be addressed to X.C. (email: cxyayd@163.com)
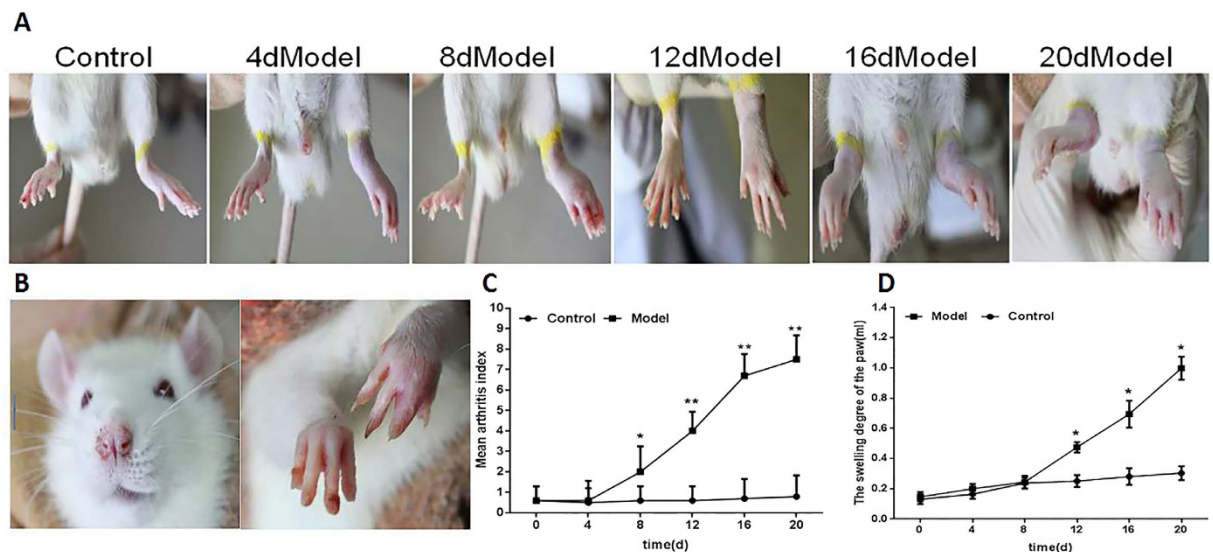
Figure 1. Arthritis induction in SD rats. (**A**) Representative images show the effect on paw edema in rats with FCA-induced arthritis. (**B**) the nose and the double fore legs inflammation secondary injury in FCA-induced SD rats. (**C**) The severity of FCA-induced arthritis in SD rats. (**D**) The swelling degree of the paw in SD rats with FCA-induced arthritis, as determined by toe swelling apparatus calculated at the indicated time points. Values are the means ± SD of at least three independent experiments. *P < 0.05; **P < 0.01 versus control. n = 15/group.

the glutathione disulfide generates glutathione with H^+ which was provided by NADPH[12]. Furthermore, some studies reported that alterations in extracellular GSH/GSSG could affect proliferation of colorectal carcinoma and lung fibroblast cells[14,15]. So the activity of GSH and GR are very important. Due to the imbalance between oxidation system and antioxidation system increased chemical reaction or insufficient antioxidant defence system results in oxidative stress[16]. Some studies suggested mitochondrial ROS (mtROS) directly regulated the composition of autophagosomes[17]. Although the regulation of autophagy is unknown, it is highly likely that it is affected by oxidative modification of transcription factors[17]. Excessive generation of ROS cause mitochondrial damage resulting in the loss of its function and then cause mitochondrial autophagy. Mitochondrial autophagy remove damaged mitochondria by preventing mtROS accumulating which is a scavenger to maintain normal mitochondrial function[18].

Resveratrol (3,5,4′-trihydroxy-trans-stilbene, Res) is a natural polyphenol abundantly found in grape skins and polygonum cuspidatum which possesses a variety of biochemical and physiological effects including anti-inflammatory, anti-oxidation, anti-proliferation and chemopreventive[18]. Low concentration of resveratrol is an excellent scavenger of hydroxyl, superoxide, and other radicals. Resveratrol is also able to avoid excessive ROS induced lipid peroxidation and DNA damage[19]. It is well known that a high dose of resveratrol can induce ovarian cancer cells apoptosis[20,21]. Silent mating-type information regulation 2 homolog 3 (Sirt3) is the primary mitochondrial deacetylase[22] and directly regulates biological functions involved in mitochondrial energy production[23] which also plays a key role in regulating mtROS homeostasis. Some seminal papers have been reported that Sirt3 regulates manganese superoxide dismutase (MnSOD) deacetylation and identified the target lysines[24–26]. At the same time, lysine acetylation is also involved in the regulation of p53 which also plays a role in mitochondrial redox regulation[27]. The study also showed that the forms of oxidative stress induce Sirt3 deacetylation activity and MnSOD activity[28]. It is well established that over expression of Sirt3 decreases both intracellular mitochondrial $O_2^{•−}$ and total ROS levels, suggesting that Sirt3 regulates both energy production and mtROS scavenging pathways[29]. Some research pointed that mitochondrial oxidative stress induced compensatory upregulation of SIRT3, which might in turn activate phosphorylation of AMPK and subsequently triggered autophagy by upregulating Beclin1 expression and LC3 II/I conversion[30]. Furthermore, Res induced apoptosis via ROS-triggered autophagy in human colon cancer cells[31], while the study indicated Res enhanced temozolomide-induced apoptotic cell death in malignant glioma by inhibiting autophagy[32]. Similarly, It is unknown whether resveratrol can regulates mtROS level to promote FLSs apoptosis by Sirt3-MnSOD axis or autophagy pathway in H_2O_2-treatment FLSs.

Results

Arthritis induction in SD rats.

The Fig. 1 displays that after the injection FCA in SD rats 20 days, compared with the secondary began to appear obvious swollen (Fig. 1A) and the nose and double fore legs appear different degree of inflammation injury (Fig. 1B). Besides, after the injection for 8, 12, 18, 20 days, compared with the control group, arthritis index was gradually increased (Fig. 1C) and the swelling degree of the paw was gradually increased, too (Fig. 1D).

Resveratrol reduces oxidative injury parameters in AA rats.

After successively intragastric administration of 5 mg/kg, 15 mg/kg and 45 mg/kg resveratrol and acetyl-l-cysteine (NAC, 200 mg/kg) for 12 days. Compared with the model group, 5 mg/kg resveratrol group of toes swelling didn't change significantly (P > 0.05).
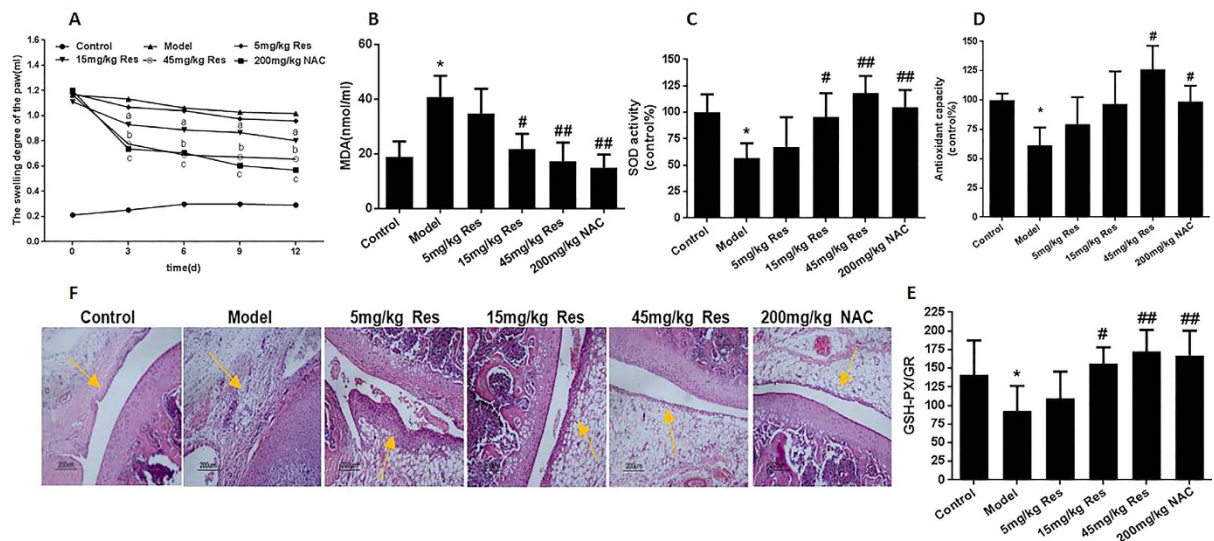
Figure 2. Resveratrol reduces oxidative injury in AA rats. after injecting FCA 20 days, treated with 5 mg/kg, 15 mg/kg, 45 mg/kg resveratrol and 200 mg/kg N-acetyl-L-cysteine (NAC) for 12 days by continuous intragastric administration. (**A**) The swelling degree of the paw in SD rats after intragastric administration. (**B**) Lipoperoxide levels in the serum from six groups rats. (**C**) SOD activity in six groups rats serum (**D**) Antioxidant capacity in six groups rats serum (**E**) The ratio of glutathione peroxidase and glutathione reductase in six groups rats serum. (**F**) HE staining of knee joint in AA rats after administration resveratrol. Data represent the means, [a]P < 0.05, [b]P < 0.01, [c]P < 0.01 versus model. Values are the means ± SD of at least three independent experiments. *P < 0.05 versus control; #P < 0.05, ##P < 0.01 versus model. n = 10/group.

But, the change of 15 mg/kg resveratrol group was significantly decreased (P < 0.05), and 45 mg/kg resveratrol and 200 mg/kg NAC group changes were most obvious (p < 0.01), after 12 days can reach 0.80 ml, 0.65 ml, 0.41 ml (Fig. 2A). And the content of MDA in the model group was about 2 folds more than control group. After administration 5 mg/kg, 15 mg/kg, 45 mg/kg resveratrol and 200 mg/kg NAC the contents of MDA were gradually decreased in rats serum (Fig. 2B). And the control of total antioxidant capacity (T-AOC) (Fig. 2C), total SOD activity (T-SOD) (Fig. 2D), the ratio of glutathione peroxidase and glutathione reductase (GSH-PX/GR) (Fig. 2E) was significantly higher than the model group. Compared with the model group, 15 mg/kg, 45 mg/kg resveratrol and 200 mg/kg NAC group was significantly increased. In model group, the synovial tissue obviously thickened, and the cartilage tissue was eroded. A large number of fragments appeared in the synovial cavity. However, after treatment with resveratrol, the above symptoms relieved or even disappeared (Fig. 2F).

Resveratrol inhibited H_2O_2-treatment FLSs proliferation. High dosage of H_2O_2 can effectively reduce the activation of FLSs. With different concentrations of H_2O_2 treatment for 12 h, we set the control group cells as 100%, $5 \mu M H_2O_2$ group increased cell activity to 111%, $10–20 \mu M$ H_2O_2 can reduce the viability to 78%, 29%. $40–80 \mu M H_2O_2$ of cell viability was only 8% (Fig. 3A). Before adding $5 \mu M H_2O_2$ treatment for 12 h, different concentrations of resveratrol pretreatment for 24 h, $50–400 \mu M$ Res can inhibit the proliferation of FLSs. $5 \mu M H_2O_2$ cell activity enhanced to 105.1%, after adding resveratrol to cells, the viability reduced to 93.2%, 80.6%, 45.2%, 32.3%, in a dose-dependent (Fig. 3B). The same, $0–10 \mu M H_2O_2$ early apoptotic cells and late apoptotic/necrotic cells with few changes. Compared with the control group, $20–80 \mu M$ H_2O_2 markedly increase early apoptotic cells and late apoptotic/necrotic cells (Fig. 3C–E). Compared with the $5 \mu M H_2O_2$ treatment group, Res also can increase $5 \mu M H_2O_2$ treatment-FLSs early apoptotic cells and late apoptotic/necrotic cells (Fig. 3C,F,G).

Resveratrol enhanced mitochondrial superoxide generation and the loss of mitochondrial membrane potential in FLSs. The effects of resveratrol on regulation of mitochondrial redox status and mitochondrial membrane potential ($\Delta\psi m$) were evaluated using MitoSOX Red (Invitrogen, USA) and assay kit with JC-1 (Life technologies, USA) in FLSs. Once MitoSOX Red reagent is selectively targeted to mitochondriain, MitoSOX Red is oxidized by $O_2^{\bullet-}$ and exhibits red fluorescence. The $5 \mu M H_2O_2$ group significantly decreased mitochondrial $O_2^{\bullet-}$ generation compared with the control group, which was notably increased by resveratrol pretreatment (Fig. 4A,C). JC-1 can selectively enter mitochondria and reversibly changes color as the $\Delta\psi m$ changes. There was a significantly increased red fluorescence in $5 \mu M H_2O_2$ group. However, Res pretreatment promoted green fluorescence generation, suggesting that the mitochondrial membrane was depolarized (Fig. 4B,D).These results suggested that resveratrol remarkably enhanced collapse of mitochondrial membrane potential in FLSs (P < 0.05).

Resveratrol declined autophagy related Beclin1 and LC3A/B proteins expression. Immunofluorescence images indicated that the control group Beclin1 protein was located in the cytoplasm and abundantly existed in the nucleus surrounding. LC3A/B protein mainly enriched in nucleus and few part
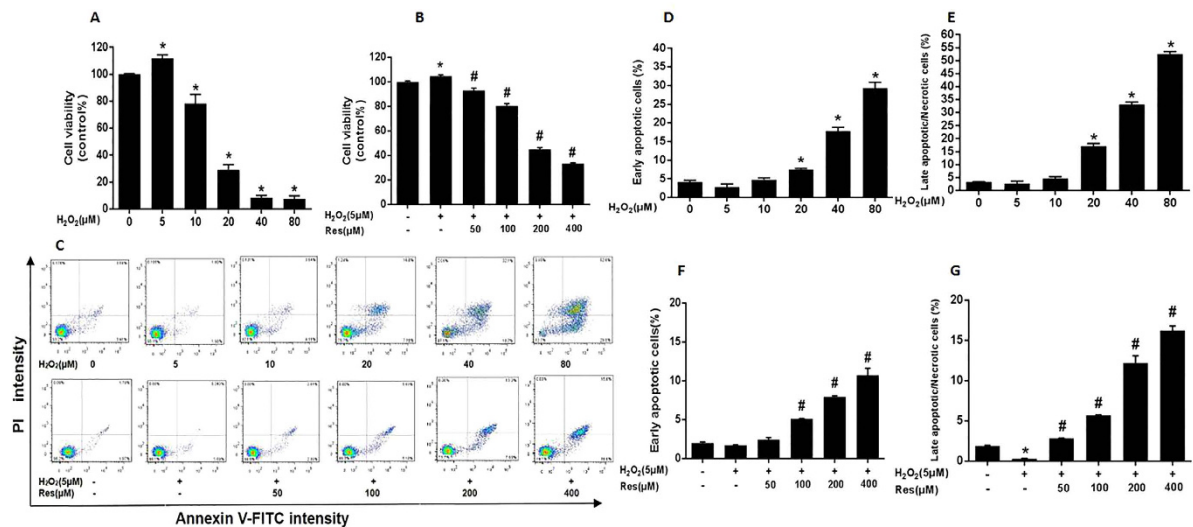
Figure 3. Resveratrol inhibited H₂O₂-treatment FLSs proliferation. (**A,B**) Cells were treated with different concentrations (0, 5, 10,20, 40 and 80 μM) H₂O₂ for 12 h and cells were pretreated for 24 h with various concentrations of Res (0, 50,100,200 and 400 μM) before treatment with 5 μM H₂O₂ incubation 12 h, respectively. Cell viability was determined using the CCK-8 assay and data are expressed as percentage of the control. (**C**) Representative images of flow cytometric analysis by Annexin V-FITC/PI staining. The bottom right quadrant represents Annexin V-FITC-stained cells (early-phase apoptotic cells) and the top right quadrant represents PI- and FITC-dual-stained cells (late-phase apoptotic or necrotic cells). (**D–G**) Quantitative determination of early apoptotic cell death as the number of Annexin V-FITC-positive cells with PI-negative cells, and late apoptotic/necrotic cell death as the number of Annexin V-FITC-positive and PI-positive cells. Values are the means ± SD of at least three independent experiments. *P < 0.05 versus control; #P < 0.05 versus 5 μM H₂O₂ group.
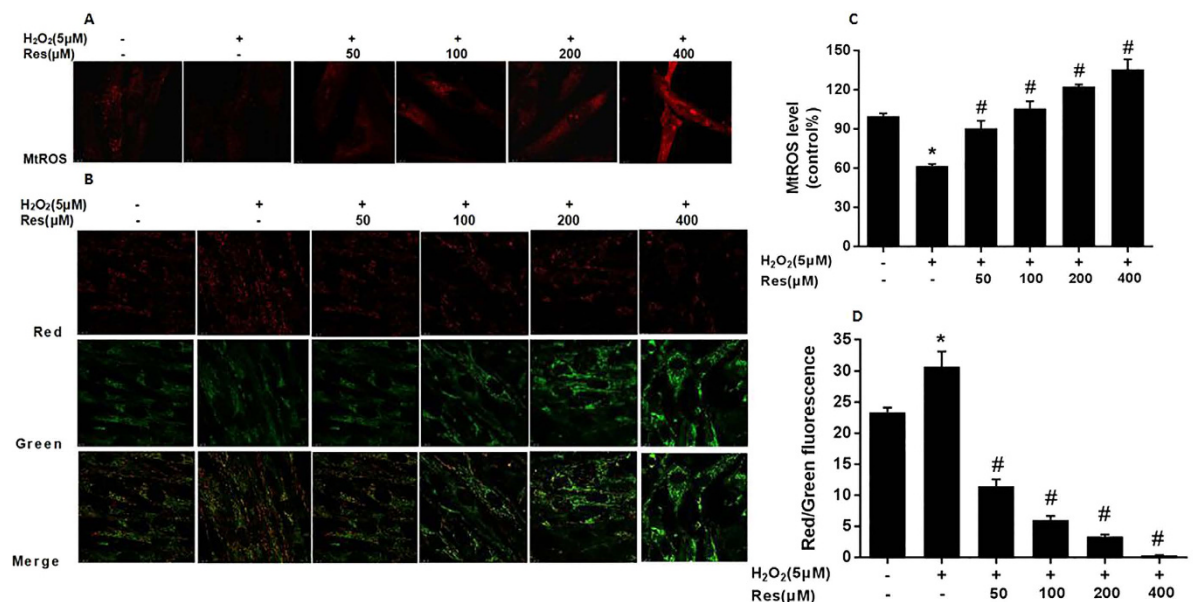

Figure 4. Resveratrol enhanced mitochondrial superoxide generation and the loss of mitochondrial membrane potential in FLSs. Cells were treated with different concentrations (0, 5, 10, 20, 40 and 80 μM) H₂O₂ for 12 h and cells were pretreated for 24 h with various concentrations of Res (0, 50, 100, 200 and 400 μM) before treatment with 5 μM H₂O₂ incubation 12 h, respectively. (**A**) The mitochondrial superoxide levels were detected using MitoSOX Red and the fluorescence images was carried out using confocal laser scanning microscopy. (**B**) Δψm was determined using confocal laser scanning microscopy. Red fluorescence represents JC-1 aggregates in normal mitochondria, whereas green fluorescence represents JC-1 monomers, indicating unhealthy mitochondria. Merged images indicate JC-1 aggregates and monomers. (**C**) The histogram show quantification of the mitochondrial superoxide levels expressed as the percentage change relative to the control group. (**D**) Δψm in each group was estimated as the red/green fluorescence. Values are the means ± SD of at least three independent experiments. *P < 0.05 versus control; #P < 0.05 versus 5 μM H₂O₂ group.
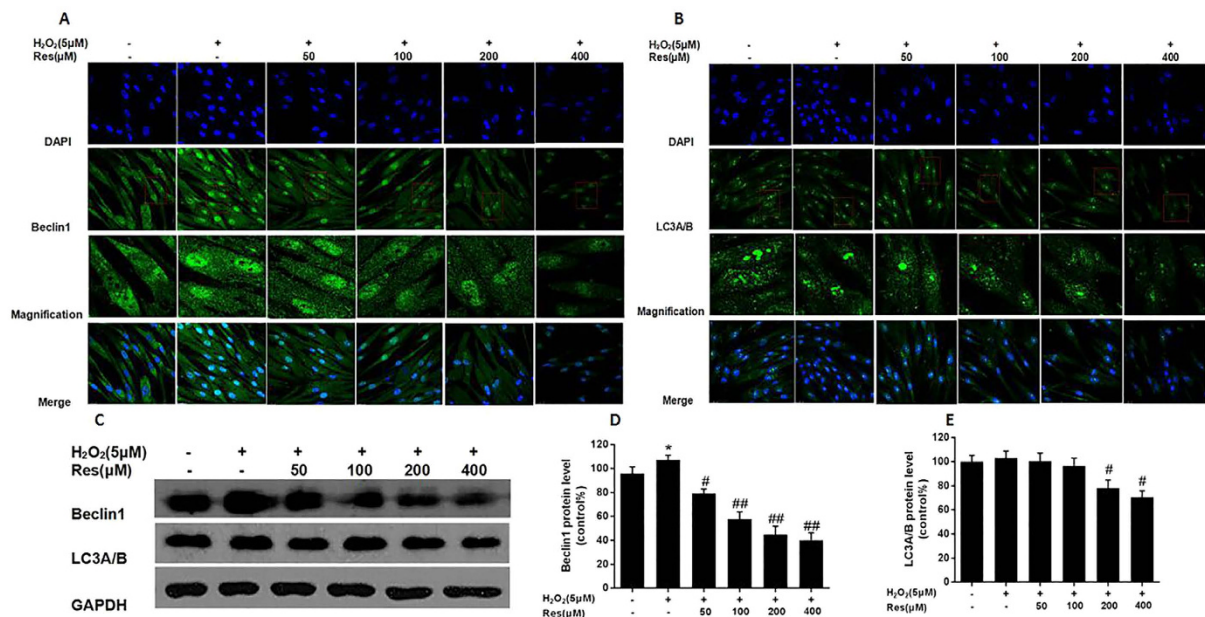
Figure 5. Resveratrol declined autophagy related Beclin1 and LC3A/B proteins expression. Cells were treated with different concentrations (0, 5, 10, 20, 40 and 80 μM) H_2O_2 for 12 h and cells were pretreated for 24 h with various concentrations of res (0, 50, 100, 200 and 400 μM) before treatment with 5 μM H_2O_2 incubation 12 h, respectively. (**A,B**) Representative images show Beclin1 and LC3A/B proteins localization in FLSs by immunofluorescence assay. Green fluorescence indicates Beclin1 and LC3A/B. Blue fluorescence indicates nucleistained with DAPI. (**C**) After the indicated treatments, the protein was harvested to detect Beclin1 and LC3A/B levels by western blot analysis. (**D,E**) Beclin1/GADPH and LC3A/B/GAPDH. Values are the means ± SD of at least three independent experiments. *$P < 0.05$ versus control; #$P < 0.05$ versus 5 μM H_2O_2 group.

presented in the cytoplasm. However, the 5 μM H_2O_2 group Beclin1 protein Mainly enriched in cytoplasm and nucleus, especially the Beclin1 fluorescence is very strong in the nucleus and with increasing concentration of Res, Beclin1 and LC3A/B fluorescence intensity gradually reduced (Fig. 5A,B). Western blot analysis, compared with control group, 5 μM H_2O_2 can increase the expression of Beclin1 and LC3A/B protein. With increasing concentration of resveratrol, the expression gradually reduced and high doses of Res protein expression level reducing is most obvious (Fig. 5C–E).

Resveratrol enhanced mtROS generation through declining mitochondrial oxdative stress related proteins SIRT3 and MnSOD expression.
Immunofluorescence images indicated that the SIRT3 protein was located in the cytoplasm and nucleus. MnSOD protein merely enriched in the cytoplasm. However, the 5 μM H_2O_2 group SIRT3 protein mainly enriched in nucleus surrounding, especially the nucleus surrounding fluorescence is very strong and with increasing concentration of Res, SIRT3 and MnSOD fluorescence intensity gradually reduced (Fig. 6A,B). Western blotting analysis, compared with control group 5 μM H_2O_2 can increase the expression of SIRT3 and MnSOD protein. With increasing concentration of Res, the expression gradually reduced and high doses of Res protein expression level reducing is most obvious (Fig. 6C–E).

Discussion
The main features of RA patients rheumatoid arthritis showed the formation of pannus invasion and destruction of articular structure in local thickening of the synovium. Pannus is mainly composed of permeate combination of synovial fibroblasts and a large number of lymphocytes and macrophages[33,34]. Human FLSs plays an important role in the pathogenesis of RA. TNF-α and IL-1β are extremely important in the induction of arthritis, can trigger the production of matrix metalloproteinases (MMPs), and ultimately damage the synovial and articular cartilage[35], In addition, macrophages and FLSs can produce proinflammatory cytokines such as TNF-α, IL-1β, IL-6, IL-8. Excessive production of pro-inflammatory cytokines stimulates neutrophils and activated macrophages the secreting ROS which making them as the medium of joint damage[36,37]. So the accumulation of ROS leads to the arthritis which is the main reason. Under the condition of oxidative stress, ROS was produced in excess leading to lipid peroxidation, protein oxidation and DNA fragmentation[38]. MDA, a marker for lipid peroxidation, is frequently used as an indicator for measurement of cellular membrane damage[39]. Superoxide anion is regulated by enzymes such as superoxide dismutase (SOD) and peroxidases, as well as endogenous supplies of antioxidants such as glutathione (GSH)[40].

Resveratrol is a phenolic compound, which is widely found in various fruits and vegetables, possess antioxidant, anti-aging, regulation of lipid metabolism, anti-cancer properties[18]. Similarly, *in vivo* experiments, it was found that the content of MDA in the model group was significantly higher than the normal group, and the
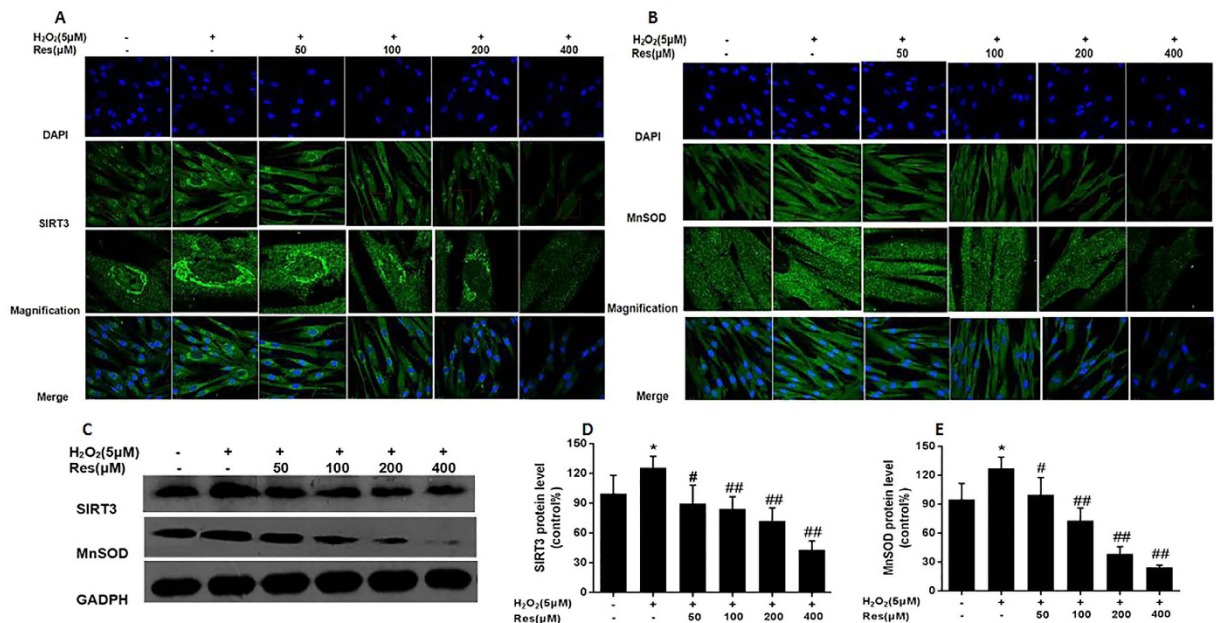
Figure 6. Resveratrol enhanced mtROS generation through declining mitochondrial oxidative stress related proteins SIRT3 and MnSOD expression. Cells were treated with different concentrations (0, 5, 10, 20, 40, 80 and 100 μM) H_2O_2 for 12 h and cells were pretreated for 24 h with various concentrations of Res (0, 50,100,200,300 and 400 μM) before treatment with 5 μM H_2O_2 incubation 12 h, respectively. (**A,B**) Representative images show mitochondrial SIRT3 and MnSOD proteins localization in FLSs by immunofluorescence assay. Green fluorescence indicates SIRT3 and MnSOD. Blue fluorescence indicates nucleistained with DAPI. (**C**) After the indicated treatments, the protein was harvested to detect SIRT3 and MnSOD levels by western blot analysis. (**D,E**) SIRT3/GADPH and MnSOD/GAPDH. Values are the means ± SD of at least three independent experiments. *$P < 0.05$ versus control; #$P < 0.05$ versus 5 μM H_2O_2 group.

5mg/kg, 15 mg/kg, 45 mg/kg resveratrol group and 200 mg/kg NAC group were significantly decreased in AA rats serum. The total SOD activity, total antioxidant capacity and the ratio of GSH-PX and GSH reductase in the 15 mg/kg resveratrol group were significantly lower than the normal control group, after successively intragastric administration of 5 mg/kg, 15 mg/kg, 45 mg/kg resveratrol and 200 mg/kg NAC, those were significantly higher. HE staining showed that 15 mg/kg, 45 mg/kg resveratrol and 200 mg/kg NAC can significantly suppressed the AA rat knee joint synovium hyperplasia, relieved the pannus formation and synovial endothelial swelling, also can effectively reduce the subsynovial layer of a large number of lymphocytes and plasma cells infiltration, inhibited synovial invasion of cartilage and subchondral substrate. Especially 45 mg/kg resveratrol improved more obviously. Thus, we further confirmed that AA rats had oxidative stress. This oxidative stress can promote the proliferation of synovial cells and the thickening of the synovial layer. However, the resveratrol could inhibit proliferation of the synovial layer in AA rats.

In recent years, more and more evidences show that resveratrol can promote the apoptosis of cancer cells[41]. High concentrations of resveratrol can induce many kinds of tumor cells apoptosis. FLSs has the characteristics of tumor like properties. Therefore, we also show that the apoptotic effect of 50–200 μM resveratrol on FLSs were not obviously, but the 200–400 μM resveratrol significantly promoted the apoptosis of FLSs, and even 400 μM of resveratrol obviously increased the apoptosis rate of FLSs. In addition, mitochondria can also regulate the apoptosis of tumor cells. In the physiological state, more than 90% of ROS are produced by the mitochondria, and in the process of respiratory chain transfer, the electron from the mitochondrial respiratory chain of the mitochondrial respiratory chain is formed by the oxidation of the complex of the oxidative phosphorylation of the complex I and III is the formation of $O_2 \bullet^-$ [42]. $O_2 \bullet^-$ mainly through manganese superoxide dismutase (MnSOD) to form H_2O_2; H_2O_2 was decomposed into H_2O by the body's hydrogen peroxide enzymes. There is a good balance between them, once the balance is broken, it will lead to the occurrence of oxidative stress, resulting in a large number of active ingredients. In our experiment, we found excessive H_2O_2 to cause early apoptotic FLSs and late apoptotic/ necrotic FLSs increasing and we also found that resveratrol can increase mtROS generation and early apoptotic cells and late apoptotic/necrotic cells in H_2O_2-treatment FLSs. So ROS plays a very important role in cell proliferation and apoptosis. At low concentrations, ROS can be used as a signal molecule to regulate cell proliferation and other functions of which can lead to cell senescence and death at high concentrations of ROS[43].

Resveratrol interferes into the signal pathway in tumor cells to regulate cell survival and apoptosis, but also regulates the mitochondrial permeability, damage the mitochondrial membrane potential[44,45], the destruction of electronic respiratory chain[46], and increase the production of mitochondrial superoxide. In our experiment, the mtROS and mitochondrial membrane potential (Δψm) were significantly increased comparing with normal

control group. With the increase of the concentration of resveratrol, and the apoptosis rate was higher. Recent studies have found that resveratrol can cause the change of SIRT3 in the SIRTs family, SIRT3 plays a key role in regulating the balance of MnSOD in cells. It is used to change the content of mitochondrial ROS by MnSOD[47]. In our experiments, $5\mu M H_2O_2$ was found to promote the expression of SIRT3 and MnSOD protein, and MnSOD protein expression decreased with the increasing resveratrol concentration, which indicated that the antioxidant capacity of SIRT3 was decreased. This also further suggests that mitochondrial ROS content is increased. This means that MtROS could trigger early apoptotic cells and late apoptotic/necrotic cells in H_2O_2-treatmnet FLSs. In addition, ROS plays a very important role in the induction of autophagy, and it is likely that transcription factors are regulated by oxidative regulation of autophagy. Recently, it was found that resveratrol can induce FLSs apoptosis in RA patients with caspase-8 and caspase-9 in the caspase pathway, which activates the caspase-3 pathway. And then, Bcl-2, Bcl-xL or Bax activity can also be changed in the mitochondrial membrane and cytoplasm, and then promote the apoptosis of cells[48]. In addition, studies have found that, under normal conditions, autophagy related proteins Beclin1, AMBRA1 and Bcl-2 or Bcl-XL combine together. When BH3-only was combined with Bcl-2 or Bcl-XL, Beclin1 and AMBRA1, VPS34 and could be formed by the combination of and VPS15, extend the wrapping of mitochondria in LC3-II under the action of mature and lysosomal binding, mitochondrial autophagy triggered[49]. In order to further understand the signal pathway of resveratrol induced apoptosis in FLSs, we studied the expression levels of LC3A/B protein and Beclin1 protein associated with autophagy maker. The results showed that after treatment with $5\mu M H_2O_2$, the expression level of LC3A/B had no significant change and the expression level of Beclin1 increased in FLSs. With different resveratrol concentration, the expression level of LC3A/B and Beclin1 decreased. Therefore, the signaling pathway of FLSs is likely to be caused by the accumulation of MtROS by autophagy pathway and oxidative stress combined action, and excessive MtROS induced apoptosis in FLSs. To sum up, resveratrol plays a very important role in the inhibition of abnormal proliferation of FLSs in AA rats, but the specific detailed mechanism of its induction of apoptosis is not clear, so the results of this study can provide a theoretical basis for the further study on the mechanism of apoptosis, and it is very important to the pathogenesis and treatment of RA.

Materials and Methods

Chemicals and reagents. Resveratrol was purchased from Aladdin (Shanghai, China). NAC (N-acetyl-L-cysteine) and Dimethyl sulfoxid (DMSO) were purchased from Sigma (St. Louis, MO, USA). The MDA assay kit, SOD activity assay kit, antioxidant capacity assay kit, glutathione peroxidase assay kit and glutathione reductase assay kit were obtained from Nanjing Jiancheng Bioengineering Institute (Nangjing, China). Dulbecco's modified eagle medium (DMEM) and fetal bovine serum (FBS) were obtained from Gibco (St Louis, MO, USA). A cell counting kit (CCK-8) was purchased from Biosharp (Hefei, China). Annexin V-FITC/PI staining kit was purchased from BestBio (Shanghai, China). Anti-MnSOD antibody, anti-Sirt3 antibody, anti-LC3A/B antibody and anti-Beclin1 antibody were purchased from Abcam (Beverly, MA, USA). Alexa Fluor 488-conjugated secondary antibody and 4′,6′-diamidino-2-phenylindole (DPI) were purchased from BEIJING BIOSS (beijing, China). MitoSOX Red mitochondrial superoxide indicator and 5,5′,6,6′-Tetrachloro-1,1′,3,3′-tetraethyl-imidacarbocyanine iodide (JC-1) for live-cell imaging was obtained from life technologies (San Diego, CA, USA).

Experimental animals and design. Male SD rats weighed $180 \pm 20\,g$ were provided from laboratory animal Center of Anhui Medical University in this experiment. Rats were acclimatized in temperature and humidity controlled rooms for one week. Rats can be freely available standard food and tap water. The left hind toe of male SD rats were injected with $150\,\mu l$ Freund's complete adjuvant (FCA, Sigma, USA) for 20 days. Control rats were injected with $150\,\mu l$ physiological saline. Then adjuvant-arthritis rats and control rats were randomly assigned to six groups treated with 5 mg/kg, 15 mg/kg, 45 mg/kg resveratrol and 200 mg/kg N-acetyl-L-cysteine (NAC, Sigma, USA) for 12 days by continuous intragastric administration. These doses have been selected based on previously described[50,51]. All animals were sacrificed after above treatment 12 days. Pairs of legs was excised, fixed in 4% paraformaldehyde or stored in $-80\,°C$ for later analysis. Blood samples were collected, and then $4\,°C$ for the night. Next day, those samples were centrifuged at 3500 rpm/min for 20 min to obtain supernatant fluid which was stored at $-80\,°C$ for further analyses.

Isolation and culture FLSs. FLSs were isolated from model group rats as described previously[52]. In brief, sterile synovial tissue were cut into $1\,mm^3$ size, with twice the volume of 0.2%-II type collagenase (Sigma, USA) which contained 10% fetal bovine serum (FBS) digesting 2 to 2.5 h (percussion one time every 30 min). And then using 0.25% trypsin digest 30 min before ending to digestion. Resuspend the cells with DMEM (Gibco, USA) containing 15% fetal bovine serum (Gibco, USA) in the $25\,cm^2$ flask, then incubated in a humidified atmosphere containing 5% CO_2 at $37\,°C$. All cells used in experiments for the 3–5 passengers.

The swelling degree of the paw and arthritis index score. The foot volume were measured before each rat left hind toe volume injected FCA. After injection occurs, every 3 or 4 days right hind foot volume measurement were executed by Toe swelling measuring instrument (ZH-YLS-7C, China). The swelling degree of the paw to calculate: swelling of the feet (ml) = model group of right hind foot volume (ml)- control group of right hind foot volume (ml) and medication after foot swelling (ml) = after administration of right hind foot volume (ml)-before administration of right hind foot volume(ml). The degree of arthritis index was determined using a scoring protocol[53], where by severity was scored on a scale of 0–4, where 0 = absent, 1 = minimal, 2 = mild, 3 = moderate, and 4 = severe.

Oxidative injury parameters. Lipid peroxidation was evaluated by means of the TBARS (thiobarbituric acid-reactive substances) assay. Malondialdehyde (MDA) comes form Lipid peroxide degradation products which can be combined with thiobarbituric acid (TBA) to form pink products. MDA content was determined

7

by using the MDA assay kit (Nanjing Jiancheng Bioengineering Institute, China) according to the manufacturer's instructions. briefly, Serum of rats with various reagents blending were incubated in 95 °C water bath for 40 min and subsequently centrifuged at 3000 rpm for 10 min to obtain supernate which was estimated absorbance by spectrophotometry at 532 nm and the values expressed as nmol (mg protein)$^{-1}$. SOD activity, Antioxidant capacity, glutathione peroxidase and glutathione reductase ratio were determined by SOD activity assay kit, antioxidant capacity assay kit, glutathione peroxidase assay kit, glutathione reductase assay kit (Nanjing Jiancheng Bioengineering Institute, Nangjing, China). Simply, serum of rats blend with reagents for several minutes. Respectively, obtaining supernate was detected absorbance by spectrophotometry at 550 nm, 520 nm, 412 nm, 340 nm and the values expressed as percentage.

Hematoxylin and eosin staining. After 12 days of continuous intragastric administration, AA rats were sacrificed. Knee-joint was harvested and fixed in 4% paraformaldehyde. Then fixed tissue was dehydrated and embedded in paraffin after 6 months of decalcification of knee joint. Knee-joint was cut into 4 micron size and mounted on glass slides. The section was stained with hematoxylin and eosin (Beyotime, Shanghai, China). Images of the stained tissue were obtained using light microscopy.

Cell growth inhibition assay. Cell viability was performed using cck-8 assays kit (Biosharp, Hefei, China) according to the manufacturer's protocols. Briefly, the cells was plated in 96-well plates and grown 24 h. Next day, the cells were treated with various concentration of hydrogen peroxide (H$_2$O$_2$) for 12 h, or after various doses of resveratrol pretreatment in FLSs for 24 h, selected dosage of H$_2$O$_2$ incubation 12 h. After above treatment, A volume of 10 μl cck-8 was added to those wells. Cells were cultured for 3 h at 37 °C. Then absorbance of the 96-well plates was determined on enzymelinked immunosorbent assay plate reader at 450 nm.

Cell apoptosis detection by flow cytometry. The apoptotic rate of FLSs was detected by flow cytometry using Annexin V-FITC/PI staining kit (BestBio, Shanghai, China) according to the manufacturer's protocol. Briefly, FLSs were seeded and incubated in 6-well plates and treated with above dosage and time.after that cells were digested with pancreatic enzymes, resuspended in 400 μl Annexin V binding buffer at a density of 1×10^6cells/ml and incubated with 5 μl Annexin V-FITC and 10 μl propidium iodide (PI) for 15 min at 4 °C in dark. Finally, cells were analyzed by flow cytometry (FACS Calibur, BD Biosciences).

MtROS assessment. The levels of mtROS were detected by MitoSOX Red Mitochondrial Superoxide Indicator (life technologies, CA, USA). FLSs were grown on glass coverslips and then harvested in 6-well plates. After treated with above dosage and time, the cells were cultured with MitoSOX Red Mitochondrial Superoxide Indicator at 37 °C for 10 min. After staining, wash the cells in fresh growth medium 3 times. Images were collected by confocal laser scanning microscope (model LEICA.SP5-DMI6000-DIC; Leica Microsystems GmbH). The quantitative analysis of the red fluorescence signal was detected by using the built-in evaluation software (Leica LAS AF Lite, Mannheim, Germany).

Mitochondrial membrane potential (Δψm) determination. Mitochondrial membrane potential (Δψm) was detected using Mitochondrial membrane potential assay kit with JC-1 (life of technology, CA, USA) according to the manufacturer's protocol. JC-1 probe was accumulated in the mitochondrial matrix polymer which gave off a strong red fluorescence in normal mitochondrion. However, JC-1 probe exists as a monomer at unhealthy mitochondrion which gave off a strong green fluorescence. The cells were grown on glass coverslips. After treated with above dosage and time, the cells were cultured with 5 μg/ml JC-1 at 37 °C for 20 min. After staining, wash the cells 3 times with PBS. The fluorescence intensity was determined by confocal laser scanning microscope (model LEICA.SP5-DMI6000-DIC; Leica Microsystems GmbH). The quantitative analysis of the red/green fluorescence signal was detected by using the built-in evaluation software (Leica LAS AF Lite, Mannheim, Germany). The Δψm was represented as the ratio of red to green fluorescence intensity.

Western blotting. Cells were seeded and incubated in 6-well plates and treated with above dosage and time and washed with ice-cold PBS and then suspended in 150 μl of RIPA lysis buffer (Beyotime, Shanghai, China). The protein concentration was determined using the BCA assay kit (Beyotime, Shanghai, China). An equal amount of proteins was added into each lane. Proteins were separated using 10% SDS-polyacrylamide gel electrophoresis (SDS-PAGE) and transferred to nitrocellulose membranes. After the membranes were blocked with 5% skim milk for 2 h, the membranes were incubated with the primary antibody overnight at 4 °C, washed with Tris-buffered saline-Tween solution (TBST) 3 times and incubated with a 1:1000 dilution of horseradish peroxidase (HRP)-labeled goat anti-rabbit IgG (Beyotime, Shanghai, China) for 1 h. Finally, bands were detected using enhanced chemiluminescence reagents (BOSTER, Wuhan, China).

Immunofluorescence staining. FLSs were grown on glass coverslips and then harvested. The coverslips were fixed with 4% (v/v) paraformaldehyde for 30 min at 37 °C and permeabilized with 0.1%Triton X-100 for 20 min at room temperature. The slides were blocked with Immunol Staining Blocking Buffer (Beyotime, Shanghai, China), incubated with anti-LC3A/B antibody, anti-MnSOD antibody, anti-Sirt3 antibody (1:200 dilution, Abcam, MA, USA), anti-Beclin1 antibody (1:300 dilution, Abcam, MA, USA) overnight at 4 °C. After washing with PBS, the slides were incubated for 40 min at 37 °C with a Alexa Fluor 488-conjugated secondary antibody (1:400 dilution; BEIJING BIOSS, Bengjing, China). Finally, the slides were washed twice with PBS and the nuclei were counterstained with 4′,6′-diamidino-2-phenylindole (DAPI, BEIJING BIOSS, Bengjing, China) for 4 min at room temperature. Images of the stained cells were obtained using confocal laser scanning microscopy (model

LEICA.SP5-DMI6000-DIC; Leica Microsystems GmbH) and the fluorescence intensity was expressed as the percentage relative to the control group (set as 100%), respectively.

Statistical analysis.   Using SPSS19.0 statistical software, data were expressed by mean $\pm$ SD. Three or more groups was compared with single factor analysis of variance (one-way ANOVA) and t test was used in the two groups. Values of $p < 0.05$ and $p < 0.01$ were considered statistically significant.

Ethics statement.   This study was approved by the Association of Laboratory Animal Sciences and the Center for Laboratory Animal Sciences at Anhui Medical University (Permit Number: 15-0026). All experiments on animals complied with the Guide for the Care and Use of Laboratory Animals by the National Institutes of Health, including all use, care and operative procedures. And all experimental procedures were followed the guidelines for humane treatment set by the Association of Laboratory Animal Sciences and the Center for Laboratory Animal Sciences at Anhui Medical University.

References

1. Bolon, B. *et al.* Rodent preclinical models for developing novel antiarthritic molecules: comparative biology andpreferred methods for evaluating efficacy. *J Biomed Biotechnol.* **569068** (2011).
2. Ward, J. R. & Jones, R. S. Studies on adjuvant-induced polyarthritis in rats. I. Adjuvant composition, route of injection, and removal of depot site. *Arthritis Rheum.* **5,** 557–564 (1962).
3. Shin, G. C. *et al.* Apigenin-induced apoptosis is mediated by reactive oxygen species and activation of ERK1/2 in rheumatoid fibroblast-like synoviocytes. *Chem Biol Interact.* **182,** 29–36 (2009).
4. Tak, P. P. & Kalden, J. R. Advances in rheumatology: new targeted therapeutics. *Arthritis Res Ther.* **13,** S5 (2011).
5. Kamanli, A. *et al.* Plasmalipid peroxidation and antioxidant levels in patients with rheumatoid arthritis. *Cell Biochem. Funct.* **22,** 53–57 (2004).
6. Seven, A., Guzel, S. & Aslan, M. & Hamuryudan, V. Lipid, protein, DNA oxidation and oxidant status in rheumatoid arthritis. *Clin. Biochem.* **41,** 538–543 (2008).
7. Raj, L. *et al.* Selective killing of cancer cells by a small molecule targeting the stress response to ROS. *Nature* **475,** 231–234 (2011).
8. DeNicola, G. M. *et al.* Oncogene-induced Nrf2 transcription promotes ROS detoxification and tumorigenesis. *Nature* **475,** 106–109 (2011).
9. Gómez, V. E., Giovannetti, E. & Peters, G. J. Unraveling the complexity of autophagy: Potential therapeutic applications in Pancreatic Ductal Adenocarcinoma. *Semin Cancer Biol.* **35,** 11–19 (2015).
10. Nash, K. M. & Ahmed, S. Nanomedicine in the ROS-mediated pathophysiology: Applications and clinical advances. *Nanomedicine.* **11,** 2033–2040 (2015).
11. Lambeth, J. D. Nox enzymes, ROS, and chronic disease: an example of antagonistic pleiotropy. *Free Radic Biol Med.* **43,** 332–347 (2007).
12. Dawane, J. S. & Pandit, V. A. Understanding redox homeostasis and its role in cancer.*J Clin Diagn Res.* **6,** 1796–1802 (2012).
13. Ushio-Fukai, M. & Nakamura, Y. *Reactive Oxygen Species and Angiogenesis: NADPH Oxidase as Target for Cancer Therapy Cancer Lett.* **266,** 37–52 (2008).
14. Ramirez, A. *et al.* Extracellular cysteine/cystine redox potential controls lung fibroblast proliferation and matrix expression through upregulation of transforming growth factor-beta. *Am J Physiol Lung Cell Mol Physiol.* **293,** L972–L981 (2007).
15. Jonas, C. R. *et al.* Extracellular thiol/disulfide redox state affects proliferation rate in a human colon carcinoma (Caco2) cell line. *Free Radic Biol Med.* **33,** 1499–1506 (2002).
16. Mateen, S. *et al.* Increased Reactive Oxygen Species Formation and Oxidative Stress in Rheumatoid Arthritis. *PLoS One.* **11,** e0152925 (2016).
17. Kubli, D. A. & Gustafsson, A. B. Mitochondria and mitophagy: the yin and yang of cell death control. *Circ Res.* **111,** 1208–1221 (2012).
18. Yu, W., Fu, Y. C. & Wang, W. Cellular and molecular effects of resveratrol in health and disease. *J Cell Biochem.* **113,** 752–759 (2012).
19. Leonard, S. S. *et al.* Resveratrol scavenges reactive oxygen species and effects radical-induced cellular responses. *Biochemical and Biophysical Research Communications.* **309,** 1017–1026 (2003).
20. Lin, H. Y. *et al.* Mechanisms of ceramide-induced COX-2-dependent apoptosis in human ovarian cancer OVCAR-3 cells partially overlapped with resveratrol. *J Cell Biochem.* **114,** 1940–1954 (2013).
21. Vergara, D. *et al.* Resveratrol downregulates Akt/GSK and ERK signalling pathways in OVCAR-3 ovarian cancer cells. *Mol Biosyst.* **8,** 1078–1087 (2012).
22. Lombard, D. B. *et al.* Mammalian Sir2 homolog SIRT3 regulates global mitochondrial lysine acetylation. *Mol. Cell. Biol.* **27,** 8807–8814 (2007).
23. Hirschey, M. D. *et al.* SIRT3 regulates mitochondrial fatty-acid oxidation by reversible enzyme deacetylation. *Nature.* **464,** 121–125 (2010).
24. Tao, R. *et al.* Sirt3-mediated deacetylation of evolutionarily conserved lysine122 regulates MnSOD activity in response to stress. *Mol Cell.* **40,** 893–904 (2010).
25. Chen, Y. *et al.* Tumour suppressor SIRT3 deacetylates and activates manganese superoxide dismutase to scavenge ROS. *EMBO Rep* **12,** 534–541 (2011).
26. Qiu, X. *et al.* Calorierestriction reduces oxidative stress by SIRT3-mediated SOD2 activation. *Cell Metab.* **12,** 62–667 (2010).
27. Sebastian, C. & Mostoslavsky, R. SIRT3 in caloriere striction: canyouhearme now? *Cell.* **143,** 667–668 (2010).
28. Someya, S. *et al.* Sirt3 mediates reduction of oxidative damage and prevention of age-related hearing loss under caloricre striction. *Cell.* **143,** 802–812 (2010).
29. Yang, H. *et al.* Design and synthesis of compounds that extend yeast replicative lifespan. *Aging Cell.* **6,** 35–43 (2007).
30. Duan, W. J. *et al.* A SIRT3/AMPK/autophagy network orchestrates the protective effects of trans-resveratrol in stressed peritoneal macrophages and RAW 264.7 macrophages. *Free Radic Biol Med.* **95,** 230–242 (2016).
31. Miki, N. *et al.* Resveratrol induces apoptosis via ROS-triggered autophagy in human colon cancer cells. *Int. J. Oncol.* **40,** 1020–1028 (2012).
32. Lipinski, M. M. *et al.* Genome-wide analysis reveals mechanisms modulating autophagy in normal brain aging and in Alzheimer's disease. *Proc. Natl. Acad. Sci. USA* **107,** 14164–14169 (2010).
33. Baier, A., Meineckel, I., Gay, S. & Pap, T. Apoptosis in rheumatoid arthritis, *Curr. Opin. Rheumatol.* **15,** 274–279 (2003).
34. Liu, H. & Pope, R. M. The role of apoptosis in rheumatoid arthritis, *Curr. Opin.Pharmacol.* **3,** 317–322 (2003).
35. Yu, D. H. *et al.* Over-expression of extracellular superoxide dismutase inmouse synovial tissue attenuates the inflammatory arthritis. *Exp Mol Med.* **44,** 529–535 (2012).
36. Comar, J. F. *et al.* Oxidative state of the liver of rats with adjuvant-induced arthritis. *Free Radic Biol Med.* **58,** 144–153 (2013).
37. Seven, A. *et al.* Lipid, protein, DNA oxidation and oxidant status in rheumatoid arthritis. *Clin Biochem.* **41,** 538–543 (2008).

38. Nash, K. M. & Ahmed, S. Nanomedicine in the ROS-mediated pathophysiology: Applications and clinical advances. *Nanomedicine*. **11,** 2033–2040 (2015).
39. Li Y. *et al.* Effect of drought and ABA on growth, photosynthesis and antioxidant system of Cotinus coggygria seedlings under two different light conditions. *Environ. Exp. Bot.* **71,** 107–113 (2011).
40. Chen, Y. R. *et al.* Direct and indirect roles of cytochrome b in the mediation of superoxide generation and NO catabolism by mitochondrial succinate-cytochrome c reductase. *J Biol Chem*. **281,** 13159–13168 (2006).
41. Alkhalaf, M. Resveratrol-induced apoptosis is associatedwith activation of p53 and inhibition of protein translationin T47D human breast cancer cells. *Pharmacology*. **80,** 134–143 (2007).
42. Lin, X., Wu, G., Huo, W. Q., Zhang, Y. & Jin, F. S. Resveratrol induces apoptosis associated withmitochondrial dysfunction in bladder carcinoma cells. *Int J Urol*. **19,** 757–764 (2012).
43. Low, I. C., Chen, Z. X. & Pervaiz, S. Bcl-2 modulates resveratrol-induced ROS production by regulating mitochondrial respiration in tumor cells. *Antioxid Redox Signal*. **13,** 807–819 (2010).
44. VanGinkel, P. R. *et al.* Resveratrol inhibits uveal melanoma tumor growth via early mitochondrial dysfunction. *Invest Ophthalmol Vis Sci*. **49,** 1299–1306 (2008).
45. Murphy, M. P. How mitochondria produce reactive oxygen species. *Biochem J*. **417,** 1–13 (2009).
46. Ma, Y. S. *et al.* Response to the increase of oxidative stress and mutation of mitochondrial DNA in aging. *Biochim Biophys Acta*. **1790,** 1021–1029 (2009).
47. Zhou, X. *et al.* Resveratrol regulates mitochondrial reactive oxygenspecies homeostasis through Sirt3 signaling pathwayin human vascular endothelial cells. *Cell Death Dis*. **5,** e1576 (2014).
48. Byun, H. S. *et al.* Caspase-8 has an essential role in resveratrol-induced apoptosis of rheumatoid fibroblast-like synoviocytes. *Rheumatology* (*Oxford*). **47,** 301–308 (2008).
49. Salminen, A., Kaarniranta, K. & Kauppinen, A. Beclin1 interactome controls the crosstalk between apoptosis, autophagy and inflammasome activation: impact on the aging process. *Ageing Res Rev*. **12,** 520–534 (2013).
50. Chen, X. Y. *et al.* Anti-inflammatory effect of resveratrol on adjuvant arthritis rats with abnormal immunological function via the reduction of cyclooxygenase-2 and prostaglandin E2. *Mol Med Rep*. **9,** 2592–2598 (2014).
51. Oliver, S. J. *et al.* Vanadate, an inhibitor of stromelysin and collagenase expression, suppresses collagen induced arthritis. *J Rheumatol*. **34,** 1802–1809 (2007).
52. Yoo, S. A. *et al.* Calcineurin is expressed and plays a critical role in inflammatory arthritis. *J. Immunol*. **177,** 2681–2690 (2006).
53. Yoo, S. A. *et al.* A novel pathogenic role of the ER chaperone GRP78/BiP in rheumatoid arthritis. *J Exp Med*. **209(4),** 871–886 (2012).

Acknowledgements

Author Contributions

W.C. and X.S. performed the proteomic data acquisition. G.W. and Z.W. analysed the proteomic data. J.Z. and J.L. performed the cell culture and relevant cell treatment. J.Z. and X.W. wrote the paper. X.C. edited the Paper. All authors reviewed the manuscript.

Additional Information